



Hydrological consequences of landscape fragmentation in mountainous northern Vietnam: Buffering of Hortonian overland flow

Alan D. Ziegler ^{a,*}, Thomas W. Giambelluca ^a, Don Plondke ^a,
Stephen Leisz ^b, Liem T. Tran ^c, Jefferson Fox ^d, Michael A. Nullet ^a,
John B. Vogler ^d, Dao Minh Troung ^e, Tran Duc Vien ^f

^a Geography Department, University of Hawaii, 2424 Maile Way SSB 445, Honolulu, HI 96822, USA

^b Institute of Geography, University of Copenhagen/Hanoi Agricultural University, Hanoi, Viet Nam

^c Department of Geography and Geology, Florida Atlantic University, Boca Raton, FL, USA

^d Environmental Studies Program, East-West Center, Honolulu, HI 96848, USA

^e Center for Natural Resources and Environmental Studies (CRES) of the Vietnam National University, Hanoi, Viet Nam

^f Center for Agricultural Research and Ecological Studies, Hanoi Agricultural University, Gia Lam, Viet Nam

Received 22 February 2006; received in revised form 27 December 2006; accepted 10 January 2007

KEYWORDS

Land-cover conversion;
Deforestation;
KINEROS2;
Swidden agriculture;
Tropical watershed hydrology;
SE Asia;
Runoff generation;
Filter strips

Summary We use a hydrology-based fragmentation index to explore the influence of land-cover distribution on the generation and buffering of Hortonian overland flow (HOF) in two disturbed upland basins in northern Vietnam (Tan Minh). Both the current degree of fragmentation in Tan Minh and the current spatial arrangement of buffers (relative to HOF source areas) provide only limited opportunities for infiltrating surface runoff from upslope source areas, in part because of the high connectivity of swidden fields on long hillslopes. The intentional placement of buffers below HOF sources and the reduction of the down-slope lengths of swidden fields could reduce the occurrence of HOF on individual hillslopes. Reduction of the total watershed total depth of HOF would require maintaining a sufficient area of buffering land covers; and this may necessitate the use of longer fallow periods. These measures are, however, counter to the land-practice trends witnessed in the last several decades (i.e., no buffers, cultivation of long slopes, and increasingly shorter fallow periods). The two most likely scenarios of future land-cover change in Tan Minh—one representing increased fragmentation, the other decreased—both lead to an increase in HOF because of reduced buffering potential. The unlikely scenario of abandonment of agriculture and subsequent regeneration of forest, leads to both less

* Corresponding author. Tel.: +1 808 956 8465; fax: +1 808 956 3512.

E-mail address: adz@hawaii.edu (A.D. Ziegler).

URL: webdata.soc.hawaii.edu/hydrology/ (A.D. Ziegler).

fragmentation and less HOF. The study highlights the hydrological impacts associated with fragmentation at Tan Minh, which is the product of decades of local and regional forcing factors that have dictated the degree and timing of timber removal and swiddening at the site.

© 2007 Elsevier B.V. All rights reserved.

Introduction

Tropical upland forests in SE Asia, South America, and Africa have increasingly become supplanted by fragmented landscapes (Skole and Tucker, 1993; Fox et al., 1995; Laurance and Bierregaard, 1997). Fragmentation is a form of land-cover conversion for which large forest tracts are replaced by irregular-sized, asymmetrical patches of remnant forest and various replacement covers (Laurance and Bierregaard, 1997). Fragmentation has often been shown to affect ecological phenomena directly (e.g., Turner, 1996; Laurance et al., 1997, 1998; Williams-Linera et al., 1998). Relatively few studies, however, have investigated the consequences of fragmentation on hydrological and climatological processes at any scale (Avissar and Peilke, 1989; Kapos, 1989; Giambelluca et al., 2003; Laurance, 2004; Ziegler et al., 2004b).

Following land-cover conversion, the physical characteristics of the replacement vegetation differ from forest at least initially (e.g., root mass/depth/turnover, total biomass, canopy characteristics including leaf area index, leaf morphology). The mechanisms and pathways that partition rainwater (viz. canopy interception, infiltration, and water ponding) on replacement land covers therefore differ from those of the undisturbed forest (Bruijnzeel, 2000, 2004; Giambelluca, 2002; Zimmermann et al., 2006). Reduced soil infiltrability, for example, is often reported on converted lands in montane areas of SE Asia (Hurni, 1982; Lal, 1987; Malmer and Gripp, 1990; Bruijnzeel and Critchley, 1994; Douglas et al., 1995; Ziegler and Giambelluca, 1997; Douglas, 1999; Sidle et al., 2006). One consequence of reduced infiltrability is an increase in Hortonian overland flow (HOF, caused when rainfall rate exceeds infiltrability and surface storage; Horton, 1933). If the spatial extent of disturbance is great enough, hydrological response is altered from that prior to land-cover conversion (cf. Bruijnzeel, 1990, 2004).

In two fragmented basins near Tan Minh Village in northern Vietnam, we found evidence that land-cover conversion increased Hortonian overland flow generation (Ziegler et al., 2004b). Saturated hydraulic conductivity (K_s) on most replacement land covers was less than that for forest. Forests in Tan Minh occupy only about 2% of the total area; and mean patch size is less than 1 ha. The remaining 2100 ha is a mosaic of more than 500 patches of various land covers differing in K_s and therefore, differing in the propensity to generate HOF. Because of the high degree of spatial heterogeneity in land cover, some portion of HOF generated on upslope areas of low K_s is infiltrated on downslope surfaces of high K_s , before entering the stream network. The extent to which 'buffering' occurs depends, in part, on the frequency that buffers are located below upslope source areas, which is inherently a function of the degree of fragmentation that has been changing over time and space in response

to both local and external factors (e.g., conservation policies, subsistence needs, market economy).

Heretofore, we have had no way of judging the potential for buffering overland flow within the fragmented landscape at Tan Minh now, nor in the past and future. In this work, we develop an index of basin-wide HOF occurrence to compare the buffering that occurs under the current degree of fragmentation with that of different scenarios of projected and historic land-cover distribution.

Study area

Tan Minh

Tan Minh (roughly 19:00°N, 104:45°E) is located west-southwest of Hanoi, in Da Bac District of Hoa Binh Province, in northern Vietnam (Fig. 1). The study area is described in more detail elsewhere (Ziegler et al., 2004b). Two watersheds comprise the study area (Fig. 2): Watershed 1 (910 ha) is located on the west side of the study area; and the larger watershed 2 (1228 ha) on the east side. Elevation range is 200–1000 m above sea level. Slopes are steep, typically 0.5–1.7 m m⁻¹; and they extend to the valley floor and/or stream channel. Bedrock is largely sandstone and schist, with some mica-bearing granite. Soils are predominantly Ultisols



Figure 1 Location of the Tan Minh study area in northern Vietnam.

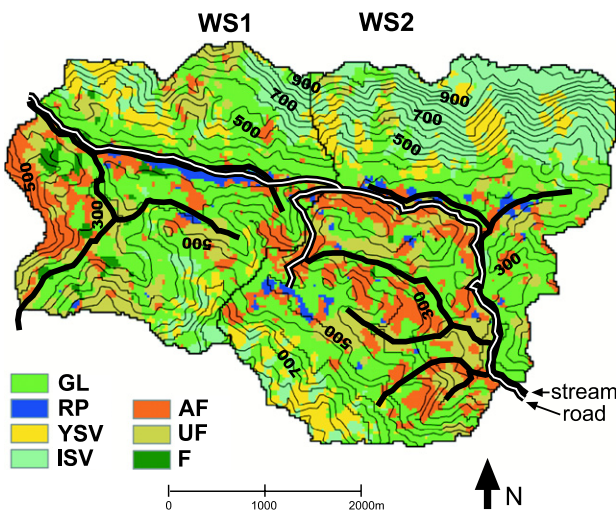


Figure 2 Land cover within watersheds (WS) 1 and 2; area and fragmentation statistics are given in Table 1. A color version is presented in Ziegler et al. (2004b). (For interpretation of the references to color in this figure legend, the reader is referred to the web version of this article.)

of the udic moisture regime. The climate is tropical monsoon, for which approximately 90% of an annual 1800 mm of rainfall occurs between May and October.

Remnant forest patches exist primarily on steep, inaccessible peaks, runs, and slopes. Some accessible hilltops and ridgelines do, however, host mature secondary forests (Fig. 3A and C). Mountain slopes are dotted with active swidden fields (Fig. 3B and D) that are farmed by Tay villagers, the primary inhabitants of Tan Minh (Fig. 3E). Juxtaposed with active fields are recently abandoned fields and various stages of secondary vegetation (mixtures of small trees, shrubs, bamboo and other grasses) that have emerged on formerly cultivated sites (Fig. 3D). In prior work (Ziegler et al., 2004b), we identified the following eight major land-cover classes based on observed physical characteristics (e.g., vegetation structure, age since cultivation): upland fields (UF), abandoned fields (AF), young secondary vegetation (YSV), grasslands (GL), intermediate secondary vegetation (ISV), forest (F), consolidated surface (CS), and paddy fields (PF). Vegetation descriptions are given in the Appendix. Table 1 lists area-related variables for the land covers without consolidated surfaces. Land-cover distribution is shown in Fig. 2. Fig. 4 shows the general sequence of land-cover evolution following clearing for shifting cultivation in Tan Minh.

Composite farming system of the Da Bac Tay

The Da Bac Tay ethnic group-referred to simply as Tay hereafter-is renown for their composite swidden farming system, which combines wet rice cultivation, swiddening



Figure 3 (A) Isolated forest fragment near the interfluvium; (B) connected fields on long, steep hillslopes; (C) mixture of various stages of secondary regrowth vegetation in an inactive swidden area; (D) abundance of young land covers, including upland fields, abandoned fields, grasslands, and other types of young secondary vegetation; (E) a Tay girl, Hian, collecting bamboo.

Table 1 Area and fragmentation-related statistics for the two watersheds investigated

Land cover	ID	Total patches	Land cover area (ha)	Relative area (%)	Mean patch area (ha)	MFA (ha)
Watershed 1						
Upland field	UF	44	162.1	17.8	3.7	9.1
Abandoned field	AF	68	126.4	13.9	1.9	11.1
Grasslands	GL	26	397.7	43.7	15.3	10.4
Young secondary vegetation	YSV	36	70.6	7.8	2.0	1.4
Intermediate secondary vegetation	ISV	29	98.1	10.8	3.4	0.6
Forest	F	24	25.1	2.8	1.0	22.3
Rice paddy	RP	16	29.8	3.3	1.9	46.2
Total	—	243	909.7	100	3.7	9.9
Watershed 2						
Upland field	UF	60	163.8	13.3	2.7	17.1
Abandoned field	AF	81	203.9	16.5	2.5	7.7
Grasslands	GL	33	408.4	33.3	12.4	12.3
Young secondary vegetation	YSV	51	131.7	10.7	2.6	1.7
Intermediate secondary vegetation	ISV	24	288.8	23.5	12.0	2.7
Forest	F	5	2.2	0.2	0.4	0.7
Rice paddy	RP	34	29.4	2.4	0.9	23.2
Total	—	288	1228.2	100	4.3	9.3

WS1 and WS2 refer to watersheds 1 and 2 (Fig. 2); MFA is mean flow accumulation; consolidated surfaces are omitted, as they are sub-grid-cell features having a total estimated areal extent of <1%.

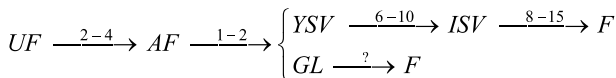


Figure 4 The general sequence of land-cover evolution following clearing for shifting cultivation in Tanh Minh. The numbers represent the approximate years to complete the transition from one land cover to another. After 2–4 years of cropping, fields are abandoned. In one instance, young secondary vegetation emerges within 2 years. This bamboo-dominated vegetation slowly matures into secondary forest within 15–25 years. Grasslands area replacement land cover, from which the timing of succession to forest we do not fully understand.

(e.g., traditionally upland rice, but now also cassava, maize, canna), home gardens, fish ponds, and the exploitation of fallow and secondary forest lands (Rambo, 1998). The swidden fields are an integral component in this composite system, which has evolved over generations or centuries (Rambo and Tran Duc Vien, 2001). The Tay began farming this region over one hundred years ago when the hillslopes were almost entirely forested. Several households now manage as many as 5–8 swiddens, which are often a mosaic of surfaces in various cultivation and fallow stages. Owing to recent intensification of cultivation in the swiddens, adjoining fields on long hillslopes are now often cultivated simultaneously (Fig. 3A).

Commencement of swiddening involves clearing of some type of advanced vegetation, including regenerating trees, bamboo, shrubs, and grasslands. Clearing is done by hand (machete) in late-March for upland rice planting. The “slash” is then allowed to dry throughout April, before burning in May. Planting is performed by hand using dibble sticks to create holes in which to place seeds. Cassava, which was introduced 40–50 years ago, is typically planted

earlier in the year. At the time of this study in 1997/98, most farmers were commonly cultivating upland rice for 1–2 years, followed by 1–2 years of cassava. Maize, canna, and ginger were also planted in a large number of swidden fields—often together. The fallow period was only 4–5 years, which is much shorter than it was when swidden agriculture was first introduced to the area a little more than 100 years ago (15–20 years).

Swiddening activities in Tan Minh can be divided into pre-cooperative (1890–1957), cooperative (1958–1988), and post-cooperative (1989–2000) periods. In general, these periods represent a progression of changes in cultivation intensity and fallow lengths over the last century. For example, during the pre-cooperative period, a swidden cycle consisted of 1–2 years of upland rice cultivation, followed by at least 15 years of fallow. During the cooperative period, 2 years of upland rice was followed by 1 year of cassava cultivation; and the fallow time decreased to about 7 years. During the recent post-cooperative period, planting of a second year of cassava has become normal—for a total of four years of cultivation; and the length of fallowing has decreased to 5 years. These generalizations are based on several prior works (Rambo, 1996; Rambo and Tran Duc Vien, 2001; Tran Duc Vien, 1997, 1998, 2003; Tran Duc Vien et al., 2004; Lam et al., 2004).

Methods

Terrain analysis

We derive topographic variables from a 30-m digital elevation model, which was created via Arc/Info version 7.3.1 (ESRI, Inc.) from a triangulated irregular network model, which was constructed from a 20-m contour topographic

Table 2 Eleven storm events recorded during the study period (3/26/98 to 6/29/98)

Storm	Date	Duration (min)	Total (mm)	Average (mm h^{-1})	$I_{1\text{-MAX}}$ (mm h^{-1})	$I_{10\text{-MAX}}$ (mm h^{-1})	$I_{30\text{-MAX}}$ (mm h^{-1})	$I_{60\text{-MAX}}$ (mm h^{-1})
1	6/4/98	686	66.8	5.8	106.7	85.3	56.9	38.9
2	5/19/98	455	28.7	3.8	76.2	45.7	32.0	22.2
3	5/28/98	136	30.7	13.6	73.0	42.7	31.5	19.9
4	6/9/98	542	38.6	4.3	76.2	45.7	30.7	22.9
5	6/7/98	86	18.3	12.8	61.0	44.2	30.5	18.1
6	5/31/98	389	21.8	3.4	121.9	44.2	26.2	13.8
7	5/18/98	48	14.2	17.8	121.9	57.9	25.4	—
8	5/5/98	119	16.5	8.3	106.7	33.0	21.3	14.8
9	5/23/98	954	42.4	2.7	45.7	27.4	19.8	16.5

Storms are ranked according to $I_{30\text{-MAX}}$ values; $I_{1\text{-MAX}}$, $I_{30\text{-MAX}}$, and $I_{60\text{-MAX}}$ refer to maximum 1-, 30- and 60-min rainfall intensities.

map. The contour map was created by digitizing the contours from a 1:50,000 scale topographic map produced by the Cartography Publishing House of Vietnam. Several features on the resulting contour map were checked against ground truth points that had been collected using GPS receivers in differential mode (horizontal accuracy ± 10 m) to confirm the accuracy of the digitized map. Through spatial analysis of land cover and topography we derive variables related to overland flow pathways and buffering phenomena in Tan Minh at a scale of 30-m. For example, we delineate watershed boundaries by determining which cells flow toward natural 'pour points', or sub-basin outlets. We then identify individual land-cover patches (groups of contiguous cells having the same land-cover type) and the number of grid cells comprising each patch. We further use Arc/Info to do the following: (1) determine flow direction from each grid cell-this is based on the relative elevation of the eight neighboring cells; and (2) derive flow-transition matrices (i.e., from which and into which land cover does surface runoff flow).

Rainfall data

We recorded one-min rainfall intensities using a MET-ONE (Grants Pass, OR) tipping bucket rain gauge (1 tip = 0.254 mm) and Campbell (Logan, UT) data logger. Although short, this period encompasses the transition from the dry to the rainy season in Tan Minh. Of a total of 49 individual rainfall events recorded during the period 26 March to 29 June 1998, we classify 11 as 'storms' using a modification of the Wischmeier and Smith (1978) criteria reported elsewhere (Ziegler et al., 2004b). The nine largest storms are ranked according to maximum 30-min rainfall intensities ($I_{30\text{-MAX}}$) in Table 2. Based on similarity in $I_{30\text{-MAX}}$ values, we assign the storms to the following groups: Large (No. 1), Medium (Nos. 2, 3, 4, 5, 6, and 7), and Small (Nos. 8 and 9).

KINEROS2

We used the event-based, physics-based KINEROS2 runoff model (Smith et al., 1995, 1999) to simulate the generation and buffering of Hortonian overland flow that occurs between two land-cover surfaces during observed storms.

Herein, we refer to these diagnostic simulations as land-cover-transition simulations ("Land-cover-transition simulations" section).

Overland flow in KINEROS2 is treated as a one-dimensional flow process, for which discharge per unit width (Q) is expressed in terms of water storage per unit area through the kinematic approximation:

$$Q = \alpha h^m \quad (1)$$

where α and m are parameters related to slope, surface roughness, and flow condition (laminar or turbulent); and h is water storage per unit area. Eq. (1) is used in conjunction with the continuity equation:

$$\frac{\partial h}{\partial t} + \frac{\partial Q}{\partial x} = q(x, t) \quad (2)$$

where x is distance downslope, t is time, and $q(x, t)$ is net lateral surface inflow rate per unit length of channel. Solution of Eq. (2) requires estimates of time- and space-dependent rainfall $r(x, t)$ and infiltration $f(x, t)$ rates:

$$q(x, t) = r(x, t) - f(x, t) \quad (3)$$

Infiltrability is defined as the limiting rate at which water can enter the soil surface (Hillel, 1971). Modeling of this process utilizes several input parameters that describe the soil profile: e.g., K_s , integral capillary drive or matric potential (G), porosity, and pore size distribution index (Brooks and Corey, 1964). The general infiltrability (f_c) equation is a function of cumulative infiltrated depth (I) (following Parlange et al., 1982):

$$f_c = K_s \left[1 + \frac{a}{e^{(al/B)} - 1} \right] \quad (4)$$

where a is a constant related to soil type (assumed to be 0.85 unless otherwise specified); and $B = (G + h_w)(\theta_s - \theta_i)$, for which h_w is surface water depth (computed internally) and the second term, unit storage capacity, is the difference of saturated (θ_s) and initial (θ_i) volumetric moisture contents (i.e., $\Delta\theta_i = \theta_s - \theta_i$). The expression $(\theta_s - \theta_i)$ is calculated as $\phi(S_{\max} - S_i)$, where ϕ is porosity, and S_{\max} and S_i are, respectively, the maximum and initial values of 'relative saturation', defined as $S = \theta/\phi$, or the fraction of the pore space filled with water. Antecedent soil moisture conditions in KINEROS2 are parameterized by assigning event-dependent values of relative saturation.

Land-cover-transition simulations

In the land-cover-transition simulations, we quantify the HOF generated on, and transported through, two adjacent upslope and downslope grid cells. The dimensions of both the upslope and downslope cells are 30 m × 30 m, thereby matching those in the Tan Minh land-cover classification and digital elevation model. The simulations focus on the six major hillslope land covers found in Tan Minh (Table 1). Paddy fields are excluded because they are inherently part of the stream network. Consolidated surfaces are not considered because they are sub-grid-cell features; the importance of these disturbed lands is discussed in the prior work (Ziegler et al., 2004b). Thus, for the six possible land covers (i.e., a total of 36 land-cover transition combinations), we calculate the depth exiting the downslope cell (HOF_{storm}, Fig. 5) for the nine storms listed in Table 2.

Before simulation, we calibrated KINEROS2 to predict runoff observed from small-scale plot experiments on an abandoned upland field in northern Thailand (Ziegler et al., 2006). Because we did not have such test data for the Vietnam field site, we used the Thailand runoff-plot data to ensure that KINEROS2 adequately simulated HOF response on an agriculture surface that is similar to the Tan Minh site. We recognize this is an important limitation, but we believe that this type of "testing" is better than none. The land-cover-transition simulations are performed by replacing parameter values from the calibration runs with those obtained from field measurements on the six hillslope land-cover types in Tan Minh (Table 1). Some of these values are the field-measured values; others are determined by comparing field observations of surface/vegetation characteristics to published values (Table 3). To ensure ample HOF generation in our simulations, we use a relative saturation value equal to the field capacity (0.67 for sandy clay loam soil, Woolhiser et al., 1990). Capillary drive was modified from the originally assigned value during model calibration.

HOF-based index of watershed-scale buffering

As a means of quantifying the degree of buffering occurring throughout a watershed for any given arrangement of land covers, we developed the following index of basin-wide HOF:

$$\text{BWHOF}_{\text{scenario}} = \frac{1}{N} \sum_{u=1}^6 \sum_{d=1}^6 T_{u,d} \times H_{u,d} \quad (5)$$

where N is the total number of basin grid-cell transitions (i.e., watershed 1 = 9,777; watershed 2 = 13,320); T is a 6x6 land-cover transition matrix containing the number of upslope grid cells of each land cover u that flow into downslope grid cells of land cover d -the set of six Tan Minh land covers for the upslope and downslope cells are the same: {AF, YSV, UF, ISV, F, GL}; H is a 6x6 matrix of HOF_{storm} values (from land-cover transition simulations, "Land-cover-transition simulations" section) calculated for every combination of upslope and downslope land covers (depicted in Fig. 5). The symbol '×' refers to standard multiplication between matrix elements.

BWHOF_{scenario} is the average HOF generated by all grid-cell transitions in a basin, for a given fragmentation scenario. It is important to remember that we are not truly simulating the flow HOF on hillslopes in the two watersheds. In essence we are assigning to every cell-to-cell transition the depth of HOF determined in the land-cover transition simulations. Therefore, no cell receives inflow from more than one upslope cell; and the simulated HOF is shallow-unconcentrated flow. No attempt is made to characterize concentrated flow entering a buffer or the convergence of flow from more than one source; thus the effects of flow accumulation are not included. BWHOF is simply a hydrologically based index that provides a means to compare how various fragmentation scenarios affect the occurrence of HOF in a location that does not have a hydrological monitoring network which would allow a distributive modeling approach.

Buffer effectiveness and fragmentation indices

To judge buffer effectiveness (BE) we define the following index:

$$\text{BE} = \frac{\text{HOF}_{\text{AF} \rightarrow \text{AF}} - \text{HOF}_{\text{AF} \rightarrow \text{buffer}}}{\text{HOF}_{\text{AF} \rightarrow \text{AF}}} \times 100\% \quad (6)$$

where HOF_{AF → AF} is KINEROS2-simulated HOF on two consecutive 30 × 30 m abandoned field grid cells (AF); and HOF_{AF → buffer} is the simulated HOF for the case that any one

Table 3 Parameters used for both buffer and land-cover-transition simulations with KINEROS2

Land cover	Code	K _s ^a (mm h ⁻¹)	C _v (-)	ϕ (-)	n (ft ^{1/6})	Ca (-)	Int (mm)
Abandoned field	AF	28	0.36	0.57	0.13	0.50	0.25
Young secondary vegetation	YSV	32	0.47	0.63	0.20	0.75	1.65
Upland field	UF	103	0.39	0.57	0.05	0.10	0.50
Intermediate secondary vegetation	ISV	67	0.58	0.55	0.20	0.80	1.75
Forest	F	63	0.49	0.61	0.15	0.85	1.80
Grasslands	GL	93	0.31	0.57	0.24	0.90	2.00

^a Variables are saturated hydraulic conductivity (K_s); the coefficient of variation for K_s(C_v); porosity (ϕ); Manning's n; vegetation coverage (Ca); total interception depth by the vegetation (Int). Manning's n is determined from field observations compared with values in Morgan (1995); Ca values are based on field surveys; Int is inferred from comparing field observations with values from Horton (1919). The following variables are the same for all land covers (based on field observations): volumetric rock fraction (1%), average microtopography relief (2 mm), average microtopography spacing (0.3 m). Common values were also used for particle density, capillary drive, and pore size distribution (see text).

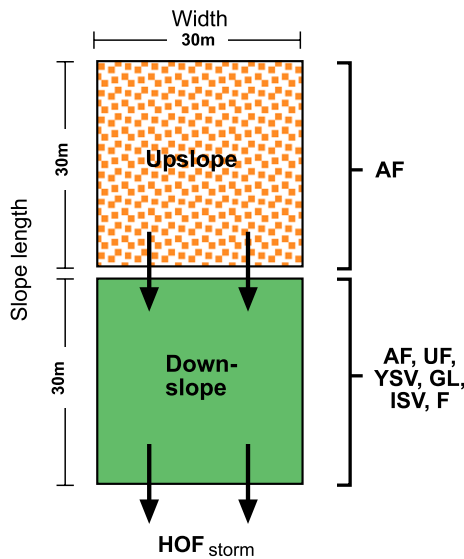


Figure 5 Depiction of $\text{HOF}_{\text{storm}}$ in the land-cover-transition simulations. $\text{HOF}_{\text{storm}}$ values, simulated for nine storms (Table 2), are used to compose the $6 \times 6 H$ matrices used to calculate BWHOF with Eq. (5). AF, YSV, UF, ISV, F, and GL are abandoned field, young secondary vegetation, upland field, intermediate secondary vegetation, forest, and grassland covers.

of the other five land covers is positioned below the abandoned field. Because the abandoned field surface has the lowest saturated hydraulic conductivity of all land covers in our classification, the $\text{AF} \rightarrow \text{AF}$ grid-cell combination generates the greatest depth of Hortonian overland flow during the land-cover-transition simulations. We therefore use $\text{HOF}_{\text{AF} \rightarrow \text{AF}}$ as the reference value to determine BE.

We define the following index of relative degree of fragmentation (RDF) to compare various fragmentation scenarios:

$$\text{RDF} = \frac{T_{\text{external}}}{T_{\text{total}}} \quad (7)$$

where T_{external} and T_{total} are, respectively, the number of external and total (internal + external) transitions in the basin. An internal transition occurs when one grid cell flows into another cell of the same land cover. External transitions represent flow into a grid cell of a differing land cover.

We define the relative degree of buffering (RDB) index as the fraction of HOF-producing cells that flow into potential buffering cells:

$$\text{RDB} = \frac{T_{\text{source} \rightarrow \text{buffer}}}{T_{\text{source}}} \quad (8)$$

where $T_{\text{source} \rightarrow \text{buffer}}$ and T_{source} are, respectively, the number of source-to-buffer transitions and total number of transitions from source cells. Source and buffer land covers are determined in the land-cover-transition simulations ("HOF sources and buffers" section). RDB is not a watershed-scale index, as it does not take into consideration infiltration of water farther downslope than one pixel. It is simply an index quantifying the frequency that buffer cells occur immediately below overland flow source cells.

Results

HOF sources and buffers

In another work, we demonstrated that abandoned fields and young secondary vegetation land covers are active HOF sources (Ziegler et al., 2004b). The land-cover-transition simulations herein show the potential role of forest, intermediate secondary vegetation, upland field, and grassland land covers as buffers. Buffer effectiveness index values are shown in Fig. 6 for the nine simulated storms (open circles; determined via Eq. (6)). This example is for the case where an upslope abandoned field flows into young secondary vegetation, upland field, intermediate secondary vegetation, forest, and grassland grid cells. The closed circles are median buffer efficiency values. Here, we use buffer efficiency values of 85% to represent the threshold effectiveness for a buffering land cover (Ziegler et al., 2006). The median buffer efficiency for upland field, intermediate secondary vegetation, forest, and grassland land covers all exceed this threshold value.

Although the buffer efficiency values for young secondary vegetation indicate a reasonable degree of buffering, it is clearly less than the other four land covers. Typically, we would not regard the upland field land cover to be either a source or buffer (Ziegler et al., 2004b). Rather, it is a hybrid, sometimes acting as a HOF source (e.g., when footpaths increase the initiation of HOF) and sometimes as a buffer (e.g., when the surface infiltration is high following hoeing or contains berms running horizontally across the slope). In the land-cover-transition simulations herein, however, upland fields function as a buffer, owing to high surface K_s .

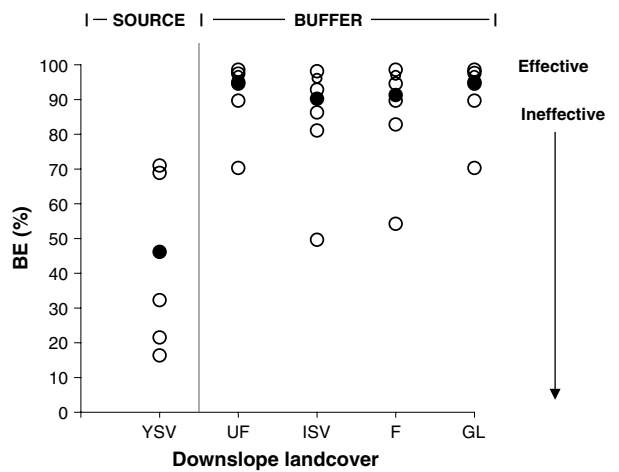


Figure 6 Buffer effectiveness (Eq. (6)) for the cases where a $30 \times 30 \text{ m}$ AF grid cell is bounded below by various types of grid cells of equal proportion. Values are calculated for all simulated storms; closed circles are median values. A buffer effectiveness value of 85% represents the threshold effectiveness for which buffer land-cover types are distinguished (Ziegler et al., 2006). YSV, UF, ISV, F, and GL are young secondary vegetation, upland field, intermediate secondary vegetation, forest, and grassland.

Land-cover-transition simulation results for example storms 1 and 4 are presented in [Table 4](#) as runoff coefficients (ROC = percentage of rainfall that becomes leaves the downslope cell has HOF, [Fig. 5](#)). Consideration of the land-cover-transition simulation results for all nine simulated storms reveal the following relationships: (1) relatively high runoff coefficients occur for source → source transitions; (2) substantial reductions in HOF occur for source → buffer transitions; (3) comparatively small depths of HOF are generated by buffer → buffer transitions; and (4) values for the buffer → source transitions largely reflect HOF generated on the downslope cell alone.

Flow transitions among land covers

Flow-transition statistics shown in [Table 5](#) indicate the frequency of flow from and flow into grid cells of each of the six hillslope land covers considered. Values along the main diagonal represent the percentage of 'internal' transitions; all other values reflect 'external' transitions to differing land covers. The percentage of external transitions indicates the degree to which a land cover is fragmented-at this scale of spatial analysis. The relative degree of fragmentation values ([Eq. \(7\)](#)) for watersheds 1 and 2 are 0.19 and 0.17, respectively. Most transitions are internal (roughly 70–90%; indicated in [Table 5](#) as 'Flows into Same'). The forest land-cover type in watershed 2 is, however, an exception (42%), reflecting the generally small size of remaining forest patches. The high percentage of internal transitions for the other land covers indicates that patch sizes are large, compared with a 30 × 30-m grid cell size. This is verified by the spatial data in that the smallest mean patch size

is 0.4 ha, or roughly 4.4 times larger than one grid cell ([Table 1](#)).

With respect to buffering potential, fewer than 30% of the source cells (abandoned fields and young secondary vegetation) flow into buffer cells (upland field, intermediate secondary fields, forest, and grassland) ([Table 5](#)). The relative degree of buffering index values ([Eq. \(8\)](#)) are 0.27 and 0.28 for watersheds 1 and 2, respectively. Grasslands, which occupy the greatest area of any single land cover, are the most abundant buffer land cover in both basins. For roughly 40–60% of all source → buffer transitions in either watershed, grasslands are the buffering land cover.

Basin-wide HOF estimates

Basin-wide HOF, calculated for watersheds 1 and 2 for the current degree of fragmentation ($BWHOF_{current}$), is compared in [Table 6](#) with that of the following three fragmentation scenarios: (1) minimum buffering ($BWHOF_{min-buffering}$); (2) maximum buffering ($BWHOF_{max-buffering}$); and (3) random distribution of land-cover cells ($BWHOF_{random}$). In the $BWHOF$ calculations for the three alternative scenarios, total basin area occupied by each land cover is the same as for the current situation; the arrangement of the various grid cells is, however, altered. All three alternative fragmentation scenarios represent higher degrees of fragmentation than the current land-cover distribution. For example, the relative degree of fragmentation ([Eq. \(7\)](#)) values for the current situation in comparison with the maximum-buffering, minimum-buffering, and random-distribution scenarios for the two watersheds are the following: watershed 1

Table 4 Runoff coefficients (KINEROS2-predicted HOF/total rainfall * 100%) during the land-cover-transition simulations for storms 1 and 4

		To source		To buffer		
		AF	YSV	ISV	F	UF
<i>(a) Storm 1</i>						
From source	AF	12.70	10.11	1.24	1.10	0.23
	YSV	10.73	7.88	0.65	0.59	0.19
From buffer	ISV	6.88	4.43	0.58	0.54	0.20
	F	6.88	4.42	0.48	0.47	0.14
	UF	6.61	4.25	0.44	0.37	0.01
	GL	6.60	4.25	0.44	0.37	0.01
<i>(b) Storm 4</i>						
From source	AF	3.07	1.65	0.12	0.09	0.09
	YSV	2.83	1.72	0.12	0.11	0.11
From buffer	ISV	1.89	1.25	0.11	0.08	0.05
	F	1.87	1.24	0.10	0.07	0.04
	UF	1.87	1.23	0.09	0.05	0.00
	GL	1.86	1.23	0.09	0.05	0.00

Values are percentages. Total rainfall depths for the two events are 66.7 and 38.6 mm, respectively ([Table 2](#)). Land cover abbreviations are the following: abandoned field (AF), young secondary vegetation (YSV), intermediate secondary vegetation (ISV), forest (F), upland field (UF), and glassland (GL).

Table 5 Flow-transition statistics for watersheds 1 and 2

	To source		To buffer				Total ^c	Flows into	
	AF ^a	YSV	ISV	F	UF	GL		Same ^b	Buffer
Watershed 1									
From source	AF	0.74	0.00	0.00	0.01	0.12	0.14	1404	0.74
	YSV	0.00	0.71	0.10	0.00	0.01	0.17	784	0.71
From buffer	ISV	0.00	0.10	0.78	0.00	0.00	0.11	1090	0.78
	F	0.10	0.00	0.00	0.68	0.08	0.14	279	0.68
	UF	0.06	0.00	0.00	0.01	0.81	0.12	1801	0.81
	GL	0.04	0.02	0.02	0.01	0.04	0.87	4419	0.87
Watershed 2									
From source	AF	0.71	0.00	0.00	0.00	0.11	0.18	2266	0.71
	YSV	0.00	0.73	0.16	0.00	0.00	0.10	1463	0.73
From buffer	ISV	0.00	0.07	0.90	0.00	0.00	0.04	3209	0.90
	F	0.08	0.00	0.00	0.42	0.17	0.33	24	0.42
	UF	0.09	0.00	0.00	0.00	0.79	0.12	1820	0.79
	GL	0.04	0.01	0.02	0.00	0.03	0.91	4538	0.91

Values indicate the percentage of transitions from one grid-cell type into another.

^a Land cover abbreviations are the following: abandoned field (AF), young secondary vegetation (YSV), intermediate secondary vegetation (ISV), forest (F), upland field (UF), and grassland (GL).

^b Flows into *Same* represents internal transitions.

^c Grid cell totals are slightly different from those that can be calculated from **Table 1** because transitions to/from paddy fields are excluded.

(0.19 versus 0.73, 0.57, and 0.72, respectively) and watershed 2 (0.17 versus 0.67, 0.75, and 0.77, respectively).

The results for each alternative scenario are presented as percentage differences from the current situation (**Table 6**). The sign reflects a positive or negative change in predicted BWHOF. Transition matrices (T in Eq. (5)) used to calculate BWHOF for the current scenario and the three alternative scenarios are presented in **Table 7**. The overland flow matrices (H) in Eq. (5) for storms 1 and 4 are derived from the data in **Table 4** by multiplying the runoff coefficient values by the total storm depths: 66.7 or 38.6 mm, respectively. The overland flow matrices for the other storms are not shown because of space limitations.

For the scenarios of minimum buffering and maximum buffering, an optimization process that manipulates the transition matrices is used to maximize BWHOF_{min-buffering} and minimize BWHOF_{max-buffering}. During optimization, we force the number of transitions both into and out of a particular land cover to equal the basin total for that land cover. Although the solutions are optimal, they are constrained by convergence, tolerance, and precision limits used by the optimization algorithm. Other 'optimal' transition matrices are possible. For the random scenario (BWHOF_{random}), transition values are assigned by multiplying the total number of grid cells of an upslope land cover by the percentage area occupied by the downslope land cover. For all hypothetical

Table 6 Estimations of basin-wide HOF in Watersheds 1 and 2 during nine storm events for the current land-cover distribution and scenarios of maximum, minimum, and random buffering

Scenario	Units	Large [†]		Medium					Small		
		1	2	3	4	5	6	7	8	9	
Watershed 1	BWHOF _{current}	mm	1.46	0.05	0.10	0.20	0.02	0.13	0.10	0.01	<0.01
	BWHOF _{max-buffering}	%	-35.3	-26.8	-27.0	-23.5	-20.1	-58.2	-19.0	-10.0	-34.0
	BWHOF _{min-buffering}	%	16.7	13.0	20.3	7.6	4.6	25.2	6.9	14.1	0.1
	BWHOF _{random}	%	-22.8	-17.7	-16.1	-16.2	-11.2	-25.6	-19.6	-2.6	4.2
Watershed 2	BWHOF _{current}	mm	1.72	0.05	0.12	0.24	0.03	0.15	0.11	0.01	<0.01
	BWHOF _{max-buffering}	%	-30.7	-20.2	-21.4	-17.5	-15.3	-43.0	-19.4	-5.9	0.0
	BWHOF _{min-buffering}	%	24.2	22.5	28.5	15.6	10.8	32.2	13.2	16.3	4.6
	BWHOF _{random}	%	-14.1	-8.5	-6.6	-8.2	-1.5	-18.8	-10.7	6.6	5.8

BWHOF_{max-buffering}, BWHOF_{min-buffering}, and BWHOF_{random} are reported as percentage changes from BWHOF_{current}; the land-cover transition matrices used to calculate BWHOF for each scenario (Eq. (5)) are listed in **Table 7**.

Table 7 Transition matrices for watersheds 1 and 2 listing the number of cells of one hillslope land cover that flow into cells of similar or different type for (a) the current distribution and three alternative fragmentation scenarios: (b) maximum buffering, (c) minimum buffering, and (d) random distribution of grid cells

	Flows into						
	AF	YSV	ISV	F	UF	GL	
<i>Watershed 1</i>							
(a) Current distribution							
RDF = 0.19; RDB = 0.27							
Flows from	AF	1032	2	0	13	167	190
	YSV	2	559	82	1	9	131
	ISV	0	114	852	3	3	118
	F	28	0	0	190	21	40
	UF	115	1	2	19	1453	211
	GL	163	95	81	53	188	3839
(b) Max-buffering							
RDF = 0.73; RDB = 1.00							
Flows from	AF	0	0	0	0	1404	0
	YSV	0	0	0	0	0	784
	ISV	0	0	811	0	0	279
	F	0	0	279	0	0	0
	UF	0	0	0	279	0	1522
	GL	1404	784	0	0	397	1834
(c) Min-buffering							
RDF = 0.57; RDB = 0.01							
Flows from	AF	620	784	0	0	0	0
	YSV	755	0	29	0	0	0
	ISV	0	0	0	279	232	579
	F	0	0	0	0	0	279
	UF	29	0	1060	0	390	322
	GL	0	0	1	0	1179	3239
(d) Random distribution							
RDF = 0.72; RDB = 0.78							
Flows from	AF	202	113	157	40	259	635
	YSV	113	63	87	22	144	354
	ISV	157	87	122	31	201	493
	F	40	22	31	8	51	126
	UF	259	144	201	51	332	814
	GL	635	354	493	126	814	1997

scenarios, upslope grid cells flow into only one down-slope cell.

The BWHOF calculations verify that buffering in Tan Minh is currently intermediate of the minimum and maximum buffering situations (Table 6). In the case of maximum buffering, predicted basin-wide HOF for eight of nine simulated storms is 6–58% lower than for the current situation. As shown in Table 7b no source → source transitions occur and source → buffer transitions are maximized (relative degree of buffering = 1.0). For the case of minimum buffering, the increase in basin-wide HOF is 5–32% for all but the smallest storm; and all available source → source transitions are selected by the optimization algorithm (relative degree of buffering = 0.0; Table 7c).

Table 7 (continued)

	Flows into						
	AF	YSV	ISV	F	UF	GL	
<i>Watershed 2</i>							
(a) Current distribution							
RDF = 0.17; RDB = 0.28							
Flows from	AF	1610	1	0	5	242	408
	YSV	2	1071	233	0	7	150
	ISV	1	212	2875	0	8	113
	F	2	0	0	10	4	8
	UF	164	4	5	4	1433	210
	GL	159	60	85	1	121	4112
(b) Max-buffering							
RDF = 0.67; RDB = 1.00							
Flows from	AF	0	0	0	0	1820	446
	YSV	0	0	0	0	0	1463
	ISV	0	0	3185	0	0	24
	F	0	0	24	0	0	0
	UF	364	1	0	23	0	1432
	GL	1902	1462	0	1	0	1173
(c) Min-buffering							
RDF = 0.75; RDB = 0.00							
Flows from	AF	803	1463	0	0	0	0
	YSV	1463	0	0	0	0	0
	ISV	0	0	0	0	1820	1389
	F	0	0	0	0	0	24
	UF	0	0	1196	1	0	623
	GL	0	0	2013	23	0	2502
(d) Random distribution							
RDF = 0.77; RDB = 0.72							
Flows from	AF	385	249	546	4	310	772
	YSV	249	161	352	3	200	498
	ISV	546	352	773	6	438	1093
	F	4	3	6	0	3	8
	UF	310	200	438	3	249	620
	GL	772	498	1093	8	620	1546

These matrices are used in the calculation of BWHOF values shown in Table 6. RDF and RDB are the relative degree of fragmentation and relative degree of buffering indices (Eqs. (7) and (8), respectively). Land cover abbreviations are the following: abandoned field (AF), young secondary vegetation (YSV), intermediate secondary vegetation (ISV), forest (F), upland field (UF), and grassland (GL).

For the BWHOF_{random} scenario, HOF occurrence is reduced because source → buffer transitions are more prevalent than for the current situation (i.e., relative degree of buffering = 0.78 versus 0.27, and 0.72 versus 0.28 for watersheds 1 and 2, respectively). Thus, in order that a higher degree of fragmentation results in a reduction in basin-wide HOF, increases in the percentage of source → buffer transitions must occur, but not necessarily at the expense of transitions that typically generate negligible HOF (i.e., buffer → buffer). While useful for judging the buffering extent associated with the current land-cover distribution, the maximum and minimum scenarios are end-member cases of plausible future land-cover distributions in Tan Minh.

Discussion

Land-cover orientation

Although patch number has increased and mean patch size has decreased substantially over the last several decades, the degree of fragmentation in the two investigated basins is less than 20% (based on the frequency of external transitions of 30×30 m grid cells). The spatial statistics indicate a predominance of 'young' land covers-young with respect to time since clearance for cultivation (Table 2): (1) active upland fields, abandoned fields, and rice paddies comprise over one-third of the total area in each basin; (2) abandoned fields represent the greatest number of individual patches (roughly 70–80), with upland fields having the second highest number of patches (roughly 40–60); (3) grasslands occupy the largest area in both watersheds (33–44%) and have the largest mean patch area (12–15 ha); and (4) lands with young secondary vegetation comprise 8–11% of the watershed area.

Although forest use and swidden agriculture have been ongoing in Tan Minh for more than a century (Fox et al., 2000), the current abundance of young land covers appears to be related to an intensification in swiddening that has taken place in the last 20–30 years. This is supported by data from a related study conducted in a 740-ha study area in the vicinity of Tan Minh (Fox et al., 2001). Between 1952 and 1995, large increases in the number of patches and decreases in mean patch size occurred for forest, secondary vegetation, and swidden land-cover classes (Fig. 7). The area occupied by open and closed forest decreased from 480 ha to 130 ha. Large area increases occurred for young land covers, particularly grasslands, secondary vegetation containing bamboo, and scrublands (Fox et al., 2001). This change is equivalent to an area increase of about 300 ha for the abandoned field, grassland, young secondary vegetation, and intermediate secondary vegetation land cover classes in the Tan Minh study area.

In addition to an increase in total lands cultivated, intensification in a swidden-based agriculture system can result in the use of shorter fallow periods while cultivating 'preferred' lands (e.g., those having richer soils, lower slope angles, or greater accessibility). The least desirable lands are

typically the ones abandoned long enough to permit recovery to forest (cf. Mather and Needle, 1998). Some remnant forest fragments in Tan Minh have never been cultivated because they are located on inaccessible terrain. If we eliminate these hard-to-access lands from consideration, more than 80% of the land area in watersheds 1 and 2 is either currently used for cropping (i.e., upland fields or rice paddies) or was in cultivation within the last 7–12 years—perhaps longer in the case of grasslands. The result of this persistent pattern of use, abandonment, and re-use is not only the fragmented landscape seen today, but one with an abundance of surfaces with high propensity to generate surface runoff (Ziegler et al., 2004b).

Flow accumulation, the total number of upslope cells that 'drain' into the destination cell, is based on slope direction and elevation of each grid cell. Mean flow accumulation therefore sheds light on where the various land-cover patches are currently located in the two basins. Young secondary vegetation, intermediate secondary vegetation, and forest land covers typically have the lowest mean flow accumulation values in Tan Minh (Table 1), indicating that these land covers are found generally at high topographic positions on or near interfluves. Few opportunities may exist for these surfaces of high infiltrability to act as buffers, except possibly for forests in watershed 2. In contrast, cultivated upland fields and recently abandoned fields have relatively high mean flow accumulation values, indicating that these surfaces are often located at lower hillslope positions. Although the upland field land cover acts as a buffer in the land-cover-transition simulations, HOF is generated frequently on paths and other disturbed areas within cultivated fields in Tan Minh (Ziegler et al., 2004b). In the cases where upland field and abandoned field surfaces are positioned on foot slopes immediately above streams, no opportunity exists for surface runoff to encounter a down-slope buffer.

Buffering in Tan Minh: present, past, future

The diagnostic land-cover simulations support the premise that if buffer patches are situated immediately downslope of HOF-producing source areas, the total depth of surface runoff generated during storms is reduced via infiltration

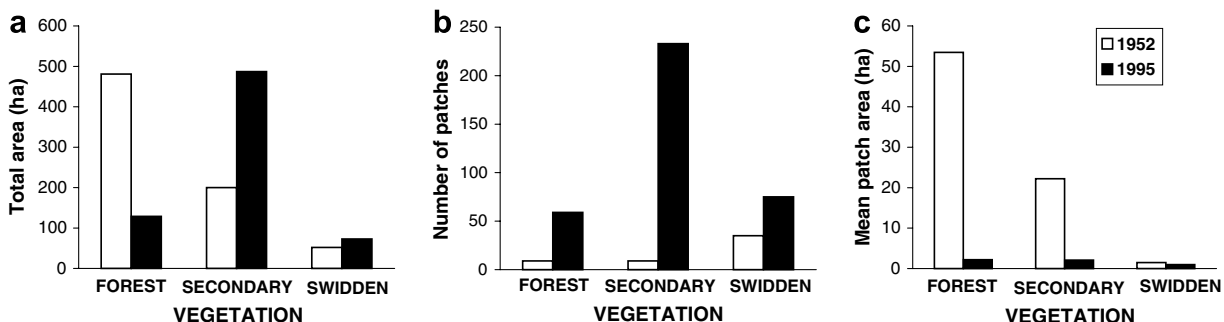


Figure 7 For the years 1952 and 1995 in the general area of Tan Minh, the following: (a) total area; (b) number of patches; and (c) mean patch size. The forest category includes open and closed-canopy forest. The secondary vegetation category includes grasslands, scrublands, and lands dominated by bamboo (most closely related to our young and intermediate vegetation classes). The swidden category is equivalent to the combination of our upland field and abandoned field categories.

(again, we are only considering shallow unconcentrated overland flow in this assessment). However, under the current degree of fragmentation, only about 30% of HOF source cells in Tan Minh flow into buffer cells. The remaining source cells flow into other sources, facilitating the formation of long flow paths that may concentrate surface runoff and compromise the effectiveness of a downslope buffer of any dimension (Fig. 3B and D; Ziegler et al., 2006). In such cases, a reduction of surface runoff could be achieved by intentionally placing vegetative buffers at intervals within long cultivated hillslopes.

Additional buffering could occur 'naturally' over time as large patches of a homogeneous HOF source land covers are divided with additional fragmentation. Fig. 8a illustrates how BWHOF could be reduced on an increasingly fragmented landscape. Beginning with the current land-cover distribution, we create a more fragmented landscape by reducing the total number of internal transitions sequentially by 10% until fragmentation approaches 100% (i.e., relative degree of fragmentation $\rightarrow 1.0$). During each iteration, the 'removed' internal transitions are divided into external transitions based on the current percentages of external transitions for each land cover. Total area occupied by each land cover does not change; only the juxtaposition and size of the patches change. For each new land-cover distribution, we calculate the corresponding relative degree of fragmentation and estimate BWHOF. For the case of 100% fragmentation (relative degree of fragmentation = 1.0), the reduction in BWHOF is 21% and 29% for watersheds 1 and 2, respectively.

Unlike the hypothetical example shown in Fig. 8a; the observed 1952–1995 land-cover changes were not random (cf. Hall et al., 1995; Hunter, 1996). They were brought about by household choices, cultural practices, communal management decisions, erratic government land management policies beginning in the 1960s, population growth, development of a reliable road network, local participation in a market economy, and a growing sense of security of local farmers to exploit forested highlands (Rambo, 1995, 1996; Le Trong Cuc and Rambo, 1999; Donovan, 1997; Fox et al., 2000, 2001; Tran Duc Vien, 2003). These types of factors had varying affects on land-use dynamics in other upland areas in both Vietnam (Castella et al., 2002; Sadoulet et al., 2002; Castella et al., 2005) and SE Asia in general (Schmidt-Vogt, 1999; Cramb, 2005; Fox and Vogler, 2005; Thongmanivong et al., 2005; Xu et al., 2005). Furthermore, these factors should continue to influence the evolution of the future landscape in Tan Minh. While a scenario of 100% fragmentation is not realistic, particularly at the $30 \times 30\text{-m}$ scale, it's likely that the degree of landscape fragmentation in Tan Minh will not remain constant.

Although land usage in Tan Minh is regulated via government policy and communal management decisions, villagers find ways to utilize non-allocated lands for subsistence and commercial purposes—even within protected areas (Donovan, 1997; Tran Duc Vien, 1997; Fox et al., 2001). Additional fragmentation would probably not occur at the expense of forest because these surfaces already occupy such a small area. Significant additional fragmentation would involve an areal increase in actively cultivated lands, and a general decrease in the length of the fallow period. The result of this scenario on BWHOF is depicted in Fig. 8b (status quo fragmentation scenario). In determining the corresponding land-cover-transition matrices for this scenario, we used the observed 1952–

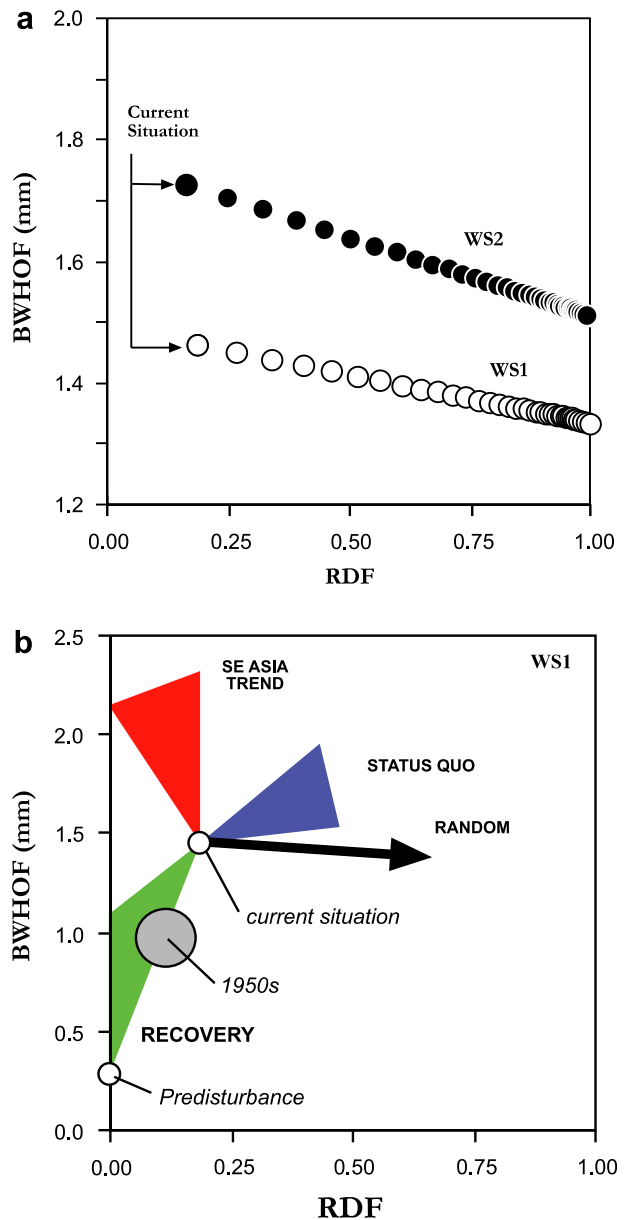


Figure 8 (a) BWHOF calculated for storm event No. 1 for an increasing relative degree of fragmentation (RDF, Eq. (7)). For each successive calculation, individual land-cover areas remain the same, but fragmentation degree increases. (b) BWHOF calculated for various land-cover change scenarios in watershed 1 for the current, past, and future situation. Random refers to the scenario shown in Fig. 8a. The recovery scenario assumes a gradual evolution back to forest following the complete abandonment of agriculture. The 1950s estimate attempts to bracket the BWHOF generated at the beginning time stamp in the Fox et al. (2000) study (i.e., summarized in Fig. 7). The pre-disturbance value was calculated for a 100% forested basin. The status quo scenario assumes fragmentation continues at rates similar to those experienced in the last 50 years (i.e., Fig. 7). The SE Asia scenario represents the change from shifting agriculture to some type of permanent cropping system. The recovery, status quo, and SE Asia trend scenarios show trajectories, rather than distinct values, owing to uncertainty in their determinations.

1995 fragmentation trends from Fox et al. (2000) to project the changes in non-forest land covers into the future. This 'status quo' fragmentation scenario is probably a more reasonable estimate of the influence of increasing fragmentation than the random scenario shown in Fig. 8a. Importantly, the predicted increase in BWHOF results largely from a reduction in the total area of the grassland land cover, which is the most prevalent buffer on the current landscape.

Abandonment of swidden-based systems has occurred recently in various locations in SE Asia (Padoch and Coffey, 2003). If this happens in Tan Minh, any one or combination of the following situations is possible:

1. Conversion of shifting fields into semi-permanent cultivation systems-examples of this include several ethnic mountain groups in northern Thailand (Schmidt-Vogt, 1999; Ziegler et al., 2004a); the Iban shifting cultivators in Sarawak (Cramb, 2005); and the Tai-Kadai groups in Lao PDR (Thongmanivong et al., 2005).
2. Giving way of shifting fields to permanent fields dedicated to a high-value crop-e.g., rubber in Xishuangbanna, China (Xu et al., 2005); cabbage in areas of northern Thailand (Delang, 2002).
3. Outward migration of young people to urban areas for wage employment, leading to a reduction in the level of intensity of agriculture (cf. Rigg and Nattapoolwat, 2001)-although this may be unlikely to occur in Tan Minh.

In Fig. 8b, we show estimates of BWHOF resulting from two more plausible land-cover change scenarios. The "SE Asia trend" scenario brackets the BWHOF values associated with conversion to permanent cropping systems, including conversion to a single high-value crop (incorporates situations 1 and 2 above). The other "recovery" scenario is based on abandonment of agriculture, allowing forest to regenerate via the evolution patterns indicated in Fig. 4. In these scenarios, fragmentation either decreases or stays at the present level, but drastically different hydrological responses result: BWHOF decreases for the recovery scenario and increases for the SE Asia trend scenario. Given the current political atmosphere, local and regional economical incentives, and population pressures, the latter scenario is likely the most plausible. Fig. 8b merely indicates plausible trajectories for changes in the occurrence of HOF in the study area.

Management issues

Forest lands, which total less than 2% of the study area, consist largely of remnant patches located at high hillslope positions; and therefore, have limited opportunities to serve as buffers. Grasslands, which occupy the largest area ($\geq 40\%$) are the most prolific buffers on the Tan Minh landscape. Currently, fewer than 30% of the HOF source cells flow into potential buffering grid cells because patch sizes of these sources are large. Our simulations support the notion that intentional placement of buffers of sufficient size on hillslopes to disrupt the connectivity of fields could reduce HOF. However, the 30-m buffers that form the basis of our analyses may be insufficient when concentrated overland flow develops during larger storms or in the case of

convergence of several flowpaths (cf. Ziegler et al., 2006). While the ideal situation would be to have a buffering land-cover situated below each HOF source, from a management perspective it is an unrealistic goal in multi-use upland basins such as those investigated in this work-especially at a 30-m scale. Managers could, however, attempt to minimize flow path lengths on surfaces where overland flow is prevalent, and avoid placing these types of surfaces directly above unprotected stream channels. Clearly more work is needed on this issue.

Limitations of BWHOF

BWHOF is simply a first-order index of hydrological disruption related to one overland flow mechanism. We focus on Hortonian overland flow because it is now more prevalent in Tan Minh than prior to the widespread occurrence of land-cover change (Ziegler et al., 2004b). Our approach is therefore a simplification of the real situation, for which saturated overland flow does occur in locations of convergence and breaks in topography. The calculation of BWHOF is based on diagnostic simulations using a common slope angle, a fixed antecedent soil moisture value, and a relatively short buffer slope lengths (30 m). The simulations results are therefore affected by assumptions made regarding several inter-related phenomena that influence model simulation of HOF on adjacent grid cells: e.g., prescribed buffer physical properties (e.g., K_s , surface roughness), soil moisture (i.e., infiltration and moisture storage do not differ for wet versus dry seasons), storm-related characteristics (i.e., intensity and duration), and type of overland flow modeled-i.e., uncentered versus concentrated flow (Ziegler et al., 2006). Importantly, the calculation of BWHOF does not include the effects of water flowing down long slope lengths. This is a significant limitation because it is this type of flow (likely concentrated) that would ultimately dictate the effectiveness of any buffer size. Finally, the 30-m scale of discretization, which was chosen to match the dimensions of the available DEM and land-cover information, is not fine enough to model the specific effects of various sub-grid-cell features that influence surface runoff generation and overland flow pathways (e.g., footpaths, rock outcrops, ditches, and berms).

Summary and conclusion

Through use of diagnostic simulations of Hortonian overland flow for each type of cell-to-cell land-cover transition, we have gained insight regarding the generation and buffering of HOF, as affected by land-cover distribution in general, and fragmentation specifically. Analysis showed that the current land-cover distribution provides less buffering than a scenario represented by a higher degree of fragmentation and a random distribution of land covers. This supports the notion that the occurrence of overland flow on the landscape is a result of decades of land-cover manipulation related to the myriad local-to-regional-scale forcing factors that have affected the study area. Although additional fragmentation could increase

overland flow buffering by as much as 20–30%, the opposite result would likely occur if cultivation continues to intensify, and the land-cover percentages shift. Because forest area is already quite low, additional fragmentation would require shortening fallow periods and dividing large patches of buffering landcovers, such as grasslands and intermediate secondary vegetation—which is the current land-use-change trend. Continuation of this trend should increase the area of surfaces having a high propensity for HOF generation (e.g., abandoned swidden fields and consolidated surfaces). Alternatively, if fragmentation were to decrease in response to shifting agriculture giving way to more permanent agriculture systems—the trend in many other areas in SE Asia—the occurrence of HOF should similarly be more frequent because sources would tend to be situated in large contiguous areas, and many buffering land cover patches would be converted to HOF source areas. The unlikely scenario of abandonment of agriculture and subsequent regeneration of forest leads to both less fragmentation and less HOF.

Acknowledgements

This paper results from joint work conducted by researchers from the University of Hawaii, East-West Center (Honolulu, HI), and Center for Natural Resources and Environmental Studies (CRES) of the Vietnam National University, Hanoi. Financial support for the Hawaii-based team was provided by a National Science Foundation Grant (No. DEB-9613613). Alan Ziegler was supported by an Environmental Protection Agency STAR fellowship. We thank the following for support during the project: Lan, Lian, Mai, and Tranh Bin Da (field work); Le Trong Cuc and Nghiêm Phuong Tuyen (CRES); J.F. Maxwell (plant taxonomy); and finally, all the Tay villagers who welcomed us in their community. An early incarnation of this paper benefited from criticisms by Sampurno Bruijnzeel (Free University Amsterdam).

Appendix. Vegetation descriptions for several land covers

Upland field (UF): Active fields, including banana (*Musa coccinea* Andr. (Musaceae), *Musa paradisiaca* L. (Musaceae)), and canna (*Canna edulis* Ker (Cannaceae)), cassava (*Manihot esculenta* Grantz (Euphorbeaceae)), corn (*Zea mays* L. (Gramineae)), and rice (*Oryza sativa* L. (Gramineae)). Weedy volunteer vegetation include *Ageratum conyzoides* L. (Compositae), *Eupatorium odoratum* L. (Compositae), *Euphorbia hirta* L. (Euphorbiaceae), *Crassocephalum crepidioides* (Bth.) S. Moore (Compositae), *Imperata cylindrica* (L.) P. Beauv. var. *major* (Nees) C.E. Hubb. ex Hubb. and Vaugh. (Gramineae), *Meliaaderazach* L. (Meliaceae), *Rorippa indica* (L.) Hiern (Cruciferae), *Saccharum spontaneum* L. (Gramineae), *Setaria palmifolia* (Korn.) Stapf var. *palmifolia* (Graminae), *Solanum verbascifolium* L. (Solanaceae), and *Urena lobata* L. ssp. *lobata* var. *lobata* (Malvaceae). Bare ground is approximately 30–50%.

Abandoned field (AF): Short grasses, herbs, and shrubs occurring on abandoned fields or lands where grazing may

limit tall vegetation growth. Species include *Helicteres angustifolia* L. (Sterculiaceae), *Imperata cylindrica*, *Microstegium vagans* (Nees ex Steud.) A. Camus (Gramineae), *Miscanthus japonicus* (Thunb.) And. (Gramineae), *Paspalum conjugatum* Beerg. (Gramineae), *Rorippa indica*, *Saccharum spontaneum*, *Litsea cubeba* (Lour.) Pers. var. *cubeba* (Lauraceae), and *Mallotus albus* M.-A. (Euphorbiaceae).

Young secondary vegetation (YSV): Evergreen broadleaf bush mixed with *nua* (*Neohouzeoua dullooa* (Gamb.) A. Camus (Gramineae, Bambusoideae)) bamboo occurring in areas where forest was once cleared. Representative species include *Acacia pennata* (L.) Willd. (Leguminosae, Mimosoideae), *Cyperus nutans* Vahl (Cyperaceae), *Rauvolfia cambodiana* Pierre ex Pit. (Apocynaceae), *Eupatorium odoratum*, *Ficus* sp. (Moraceae), *Microstegium vagans*, *Saccharum spontaneum*, and *Urena lobata*.

Grassland (GL): Tall grasslands occurring where forest has been cleared and, perhaps, the land overworked during farming. Three species dominating this land cover, *Imperata cylindrica*, *Thysanolaena latifolia* (Roxb. ex Horn.) Honda (Gramineae) and *Saccharum spontaneum*, often reach heights exceeding 2–3 m and have extensive root systems that help them regenerate quickly after fire. Other common species are *Eupatorium odoratum*, *Microstegium vagans*, and *Urena lobata*.

Intermediate secondary vegetation (ISV): One-story ‘forest’ dominated by two bamboo species: *nua* and *giang* (*Ampelocalamus patellaris* (Gamb. Emend. Stap.) Stap. (Gramineae, Bambusoideae)). Other representative species include *Alpinia blepharocalyx* K. Sch. (Zingiberaceae), *Vernicia Montana* Lour. (Euphorbiaceae), *Cyperus nutans*, *Livistona saribus* (Lour.) Chev. (Palmae), *Pteris vittata* L. (Pteridaceae), and *Styrax tonkinensis* (Pierre) Pierre ex Guill. (Styracaceae). The understory is composed primarily of bamboo litter and shoots emerging from extensive root systems.

Forest (F): Disturbed evergreen broadleaf forest, attaining heights of 25–30 m. The discontinuous upper (25–30 m) and complex secondary (8–25 m) stories include the following representative tree species: *Heteropanax fragrans* (Roxb.) Seem. (Araliaceae), *Vernicia Montana*, *Alphonsea tonkinensis* A. DC. (Annonaceae), *Melicope pteleifolia* (Champ. ex Bth.) T. Hart. (Rutaceae), *Garcinia planchonii* Pierre (Guttiferae), *Ostodes paniculata* Bl. (Euphorbiaceae), *Archidendron clypearia* (Jack) Niels. ssp. *clypearia* var. *clypearia* (Leguminosae, Mimosoideae), and *Schefflera heptaphylla* (L.) Frod. (Araliaceae). A bushy understory (2–8 m) and the forest floor includes *Breynia retusa* (Denn.) Alst. (Euphorbiaceae), *Bridelia hermandii* Gagnep. (Euphorbiaceae), *Cyperus nutans*, *Dioscorea depauperata* Prain and Burk. (Dioscoreaceae), *Rauvolfia cambodiana*, *Ficus variegata* Bl. (Moraceae), *Livistona saribus*, *Miscanthus japonicus*, *Ostodes paniculata* Bl. (Euphorbiaceae), *Phrinium capitatum* Lour. (Marantaceae), *Psychotria rubra* (Lour.) Poir. (Rubiaceae), and *Selaginella monospora* Spring (Selaginellaceae).

References

- Avissar, R., Peilke, R.A., 1989. A parameterization of heterogeneous land-surface for atmospheric numerical models and its

- impact on regional meteorology. *Month. Weath. Rev.* 117, 2113–2136.
- Brooks, R.H., Corey, A.T., 1964. Hydraulic properties of porous media. *Hydrology paper 3*, Colorado State University, Fort Collins, CO.
- Bruijnzeel, L.A., 1990. *Hydrology of Moist Tropical Forest and Effects of Conversion: A State of Knowledge Review*. IHP-UNESCO Humid Tropical Programme, Paris.
- Bruijnzeel, L.A., 2000. Forest hydrology. In: Evans, J.C. (Ed.), *The Forests Handbook*. Blackwell Scientific, Oxford, UK (Chapter 12).
- Bruijnzeel, L.A., 2004. Hydrological functions of tropical forests: not seeing the soil for the trees? *Agri. Ecosys. Environ.* 104, 185–228.
- Bruijnzeel, L.A., Critchley, W.R.S., 1994. Environmental impacts of logging moist tropical forests. In: *International Hydrology Programme, Series 7*, Paris, UNESCO.
- Castella, J.-C., Gevraise, V., Novosad, P., Pham, H.M., 2002. Centralized planning and agricultural policy: the role of the state in the agrarian dynamics of Duc Van commune, Ngan Son District, Bac Kan Province, Viet Nam. In: Castella, J.C., Dang, K.Q. (Eds.), *Doi Moi in the Mountains, Land use changes and farmers' livelihoods strategies in Bac Kan Province, Vietnam*. The Agriculture Publishing House, Ha Noi, Viet Nam, pp. 99–119.
- Castella, J.-C., Pham, H.M., Suan, P.K., Villano, L., Tronche, N.R., 2005. Analysis of village accessibility and its impact on land use dynamics in a mountainous province of northern Vietnam. *Appl. Geog.* 25, 308–326.
- Cramb, R.A., 2005. Farmers' strategies for managing acid upland soils in Southeast Asia: an evolutionary perspective. *Agri. Ecosys. Environ.* 106, 69–87.
- Delang, C., 2002. Deforestation in Northern Thailand: the result of Hmong Farming Practices or Thai development strategies? *Soc. Nat. Resour.* 15, 483–501.
- Donovan, D., 1997. Development in the local context: case studies from selected hamlets in five northern provinces. In: Donovan, D., Rambo, A.T., Fox, J., Le Trong Cuc, Tran Duc Vien, Tran Duc (Eds.), *Development Trends in Vietnam's Northern Mountain Region. Case Studies and Lessons from Asia*, vol. 2. National Political Publishing House, Hanoi.
- Douglas, I., 1999. Hydrological investigations of forest disturbance and land cover impacts in South-East Asia: a review. *Philos. Trans. Roy. Soc. Biol. Sci.* 354 (1391), 1721–1897.
- Douglas, I., Greer, T., Sinun, W., Anderton, S., Bidin, K., Spilsbury, M., Suhaimi, J., Sulaiman, A.B., 1995. Geomorphology and rainforest logging practices. In: McGregor, D.F.M., Thompson, D.A. (Eds.), *Geomorphology and Land Management in a Changing Environment*. Wiley, Chichester, UK, pp. 309–320.
- Fox, J., Vogler, J.B., 2005. Land-use and land-cover change in montane mainland southeast Asia. *Environ. Manage.* 36, 394–403.
- Fox, J., Krummel, J., Yarnasarn, S., Ekasingh, M., Podger, N., 1995. Land use and landscape dynamics in northern Thailand: assessing change in three upland watersheds. *Ambio* 24, 328–334.
- Fox, J., Minh Troung, Dao, Rambo, A.T., Nghiem Phuong Tuyen, Le Trong Cuc, Leisz, S., 2000. Shifting cultivation: a new old paradigm for managing tropical forests. *BioScience* 50, 521–528.
- Fox, J., Leisz, S., Minh Troung, Dao, Rambo, A.T., Nghiem Phuong Tuyen, Le Trong Cuc, 2001. Shifting cultivation without deforestation: a case study in the mountains of northwestern Vietnam. In: Millington, A.C., Walsh, S.J., Osborne, P.E. (Eds.), *Applications of GIS and Remote Sensing in Biogeography and Ecology*. Kluwer Academic Publishers, Boston, MA.
- Giambelluca, T.W., 2002. Hydrology of altered tropical forests. *Hydrol. Process.* 16, 1665–1669.
- Giambelluca, T.W., Ziegler, A.D., Nullet, M.A., Dao, T.M., Tran, L.T., 2003. Transpiration in a small tropical forest patch. *Agri. Forest Meteorol.* 117, 1–22.
- Hall, C.A.S., Tian, H., Qi, Y., Pontius, G., Cornell, J., 1995. Modelling spatial and temporal patterns of tropical land use change. *J. Biogeog.* 22, 753–757.
- Hillel, D., 1971. *Soil and Water – Physical Principles and Processes*. Academic Press, New York.
- Horton, R.E., 1919. Rainfall interception. *Month. Weath. Rev.* 47, 603–623.
- Horton, R.E., 1933. The role of infiltration in the hydrologic cycle. *Eos Trans. AGU* 14, 446–460.
- Hunter, 1996. *Fundamentals of Conservation Biology*. Blackwell Science, Cambridge, MA.
- Hurni, H., 1982. Soil erosion in Huai Thung Choa-northern Thailand. Concerns and constraints. *Mount. Res. Develop.* 2, 141–156.
- Kapos, V., 1989. Effects of isolation on the water status of forest patches in the Brazilian Amazon. *J. Trop. Ecol.* 5, 173–185.
- Lal, R., 1987. *Tropical Ecology and Physical Edaphology*. Wiley, New York.
- Lam, N.T., Patanothai, A., Rambo, A.T., 2004. Recent changes in the composite swidden farming system of a Da Bac Tay ethnic minority community in Vietnam's northern mountain region. *SE Asian Studies* 42, 273–293.
- Laurance, W.F., 2004. Forest-climate interactions in fragmented tropical landscapes. *Phil. Trans. Roy. Soc. Lond. B* 359, 345–352.
- Laurance, W.F., Bierregaard Jr., R.O., 1997. Preface: a crisis in the making. In: Laurance, W.F., Bierregaard, J.O., Jr.Jr. (Eds.), *Tropical Forest Remnants: Ecology, Management, and Conservation of Fragmented Communities*. University of Chicago Press, Chicago.
- Laurance, W.F., Laurance, S.G., Ferreira, L.V., Rankin-de Merona, J.M., Gascon, C., Lovejoy, T.E., 1997. Biomass collapse in Amazonian forest fragments. *Science* 278, 1117–1118.
- Laurance, W.F., Ferreira, L.V., Rankin-de Merona, J.M., Laurance, S.G., 1998. Rain forest fragmentation and the dynamics of Amazonia tree communities. *Ecology* 79, 2032–2040.
- Le Trong Cuc, Rambo, A.T., 1999. Composite Swidden farmers of Ban Tat: A case study of the environmental and social conditions in a Tay Ethnic Minority Community in Hoa Binh Province, Vietnam. In: Center for Natural Resources and Environmental Studies (CRES), Vietnam National University, Hanoi.
- Malmer, A., Gripp, H., 1990. Soil disturbance and loss of infiltrability caused by mechanized and manual extraction of tropical rainforest in Sabah, Malaysia. *Forest Ecol. Manage.* 38, 1–12.
- Mather, A.S., Needle, C.L., 1998. The forest transition: a theoretical basis. *Area* 30, 117–124.
- Morgan, R.P.C., 1995. *Soil Erosion and Conservation*. Longman Group Limited, Essex, UK.
- Padoch, C., Coffey, K., 2003. Monitoring the demise of swidden in Southeast Asia: local realities and regional ambiguities. In: *Local Land use Strategies in a Globalizing World: Shaping Sustainable Social and Natural Environments*, Proceedings of the International Conference, August 21–23, 2003, Institute of Geography, University of Copenhagen, Denmark.
- Parlange, J.-Y., Lisle, I., Braddock, R.D., Smith, R.E., 1982. The three-parameter infiltration equation. *Soil Sci.* 133, 337–341.
- Rambo, A.T., 1995. Defining highland development challenges in Vietnam. In: Rambo, A.T., Reed, R.R., Le Trong Cuc, DiGregorio, M.R. (Eds.), *The Challenge of Highland Development in Vietnam*. Program on Environment, East-West Center, Honolulu, HI.
- Rambo, A.T., 1996. The composite swiddening agroecosystem of the Tay ethnic minority of the northwestern mountain of Vietnam. In: Rerkasem, B. (Ed.), *Montane Mainland Southeast Asia in Transition*, Chiang Mai University Consortium, Chiang Mai Thailand, pp. 69–89.
- Rambo, A.T., Tran Duc Vien, 2001. Social organization and the management of natural resources: a case study of Tat Hamlet, a Da Bac Tay ethnic minority settlement in Vietnam's northwestern mountains. *SE Asian Studies* 39, 299–324.
- Rigg, J., Nattapoolwat, S., 2001. Embracing the global in Thailand: activism and pragmatism in an era of deagrarianization. *World Dev.* 29 (6), 945–960.

- Sadoulet, D., Castella, J.-C., Vu, H.N., Dang, D.Q., 2002. A short history of land use change and farming system differentiation in Xuat Hoa Commune, Bac Kan, Province, Viet Nam. In: Castella, J.C., Dang, K.Q. (Eds.), *Doi Moi in the Mountains, Land use Changes and Farmers' Livelihoods Strategies in Bac Kan Province, Vietnam*. The Agriculture Publishing House, Ha Noi, Viet Nam, pp. 21–46.
- Schmidt-Vogt, D., 1999. Swidden Farming and Fallow Vegetation in Northern Thailand, *Geocological Research*, vol. 8. Franz Steiner Verlag, Stuttgart, Germany.
- Sidle, R.S., Ziegler, A.D., Negishi, J.N., Abdul Rahim, N., Siew, R., 2006. Erosion processes in steep terrain – truths, myths, and uncertainties related to forest management in Southeast Asia. *Forest Ecol. Manage.* 224, 199–225.
- Skole, D., Tucker, C., 1993. Tropical deforestation and habitat fragmentation in the Amazon: satellite data from 1978 to 1988. *Science* 260, 1905–1910.
- Smith, R.E., Goodrich, D.C., Quinton, J.N., 1995. Dynamic, distributed simulation of watershed erosion: the KINEROS2 and EUROSEM models. *J. Soil Water Cons.* 50, 517–520.
- Smith, R.E., Goodrich, D.C., Unkrich, C.L., 1999. Simulation of selected events on the Catsop catchment by KINEROS2 A report for the GCTE conference on catchment scale erosion models. *Catena* 37, 457–475.
- Thongmanivong, S., Fujita, Y., Fox, J., 2005. Resource use dynamics and land-cover change in Ang Nhai and Phou Phanang National Forest Reserve, Lao PDR. *Environ. Manage.* 36, 382–393.
- Tran Duc Vien, 1997. Soil erosion and nutrient balance in swidden fields of the Da Bac District, Vietnam. Report No. 10667, Program on Environment, East-West Center, Honolulu HI.
- Tran Duc Vien, 1998. Soil erosion and nutrient balance in swidden fields of the composite swiddening agroecosystem in the northwestern mountains of Vietnam. In: Paranothai, A. (Ed.), *Land Degradation and Agricultural Sustainability: Case Studies from Southeast and East Asia*. Regional Secretariat, the Southeast Asian Universities Agroecosystem Network (SUAN). Khan Kaen University, Thailand.
- Tran Duc Vien, 2003. Culture, environment, and farming systems in Vietnam's northern mountain region. *SE Asian Studies* 41, 180–205.
- Tran Duc Vien, Dung, Dung, Nguyen Van, Dung, Pham Tien, Lam, Nguyen Thanh, 2004. A nutrient balance analysis of the sustainability of a composite swiddening agroecosystem in Vietnam's northern mountain region. *SE Asian Studies* 41, 491–502.
- Turner, I.M., 1996. Species loss in fragments of tropical rain forest: a review of the evidence. *J. Appl. Ecol.* 33, 200–209.
- Williams-Linera, G., Domiguez-Gastelu, V., Garcia-Zurita, M.E., 1998. Microenvironment and floristics of different edges in a fragmented tropical rainforest. *Cons. Biol.* 12, 1091–1102.
- Wischmeier, W.H., Smith, D.D., 1978. Predicting Rainfall Erosion Losses, Agriculture Handbook No. 53, USDA, Washington, DC.
- Woolhiser, D.A., Smith, R.E., Goodrich, D.A., 1990. KINEROS, A Kinematic Runoff and Erosion Model: Documentation and User Manual, USDA-Agricultural Research Service, ARS-77.
- Xu, J.C., Fox, J., Vogler, J.B., Peifang, Zhang, Yongshou, Fu, Lixin, Yang, Jie, Qian, Leisz, S., 2005. Land-use and land-cover change and farmer vulnerability in Xishuangbanna Prefecture in south-western China. *Environ. Manage.* 36, 404–413.
- Ziegler, A.D., Giambelluca, T.W., 1997. Importance of rural roads as source areas for runoff in mountainous areas of northern Thailand. *J. Hydrol.* 196, 204–229.
- Ziegler, A.D., Giambelluca, T.W., Sutherland, R.A., Nullet, M.A., Yarnasarn, S., Pinthong, J., Preechapanya, P., Jaiarree, S., 2004a. Toward understanding the cumulative impacts of roads in agricultural watersheds of Montane Mainland Southeast Asia. *Agri. Ecosys. Environ.* 104, 145–158.
- Ziegler, A.D., Giambelluca, T.W., Tran, L.T., Vana, T.T., Nullet, M.A., Fox, J., Tran Duc Vien, Pinthong, J., Maxwell, J.F., Evett, S., 2004b. Hydrological consequences of landscape fragmentation in mountainous Northern Vietnam: evidence of accelerated overland flow generation. *J. Hydrol.* 287, 124–146.
- Ziegler, A.D., Tran, L.T., Sidle, R.C., Giambelluca, T.W., Sutherland, R.A., Tran Duc Vien, 2006. Effective slope lengths for buffering hillslope surface runoff in fragmented landscapes in northern Vietnam. *Forest Ecol. Manage.* 224, 104–118.
- Zimmermann, B., Elsenbeer, H., De Moraes, J.M., 2006. The influence of land-use changes on soil hydraulic properties: implications for runoff generation. *Forest Ecol. Manage.* 222, 29–38.